A Simulation Approach to the Two-point Stochastic Model of Olfactory Neurons

P. MARŠÁLEK

Department of Pathological Physiology, First Medical Faculty, Charles University, U nemocnice 5, 128 53 Praha 2, Czech Republic

Abstract. Neurons need two basic properties to carry out their functions. The first is their ability to transduce the changes of the dendritic potential and to sum them in spatial and temporal dimensions. The second is their ability to elicit an action potential which can be transmitted along the axon at a long distance. This simulation study demonstrates how these two properties can be retracted to the two points of the neuron model. First we discussed the definition and general properties of the so-called two-point or spiking neuron model. Then a simple simulated solution of the first passage time problem of the birth and death process applied in this model was discussed. In case of olfactory cells, the model exhibited a behaviour similar to the experimental data with parameter values corresponding to the suprathreshold concentrations of an odorant.

Key words: Two-point model — Birth and death process — Computer simulation

Introduction

In recent studies the attention has been focused on questions concerning the function of a single neuron. The family of known ion channels grows more and more branched. There is a large number of toxins available for blocking these channels (Witkovsky 1989). Changes of the electric potential at neuronal membranes are described by classical Hodgkin and Huxley partial differential equations (Tuckwell 1988b). This system of equations does not yield too different solutions when a greater number of ion channels and their biophysical properties are introduced. More exact data on the ultrastructural organization of neurons are now available. The direct data input from picture processing and picture analysis systems gives a more solid background for estimating the single neuron function. Computational reasons lead to simplifications of rigorous deterministic descriptions of the function of the membrane. According to Tuckwell, " a stochastic version of nonlinear systems of equations such as those of Hodgkin and Huxley is a mathematically formidable task" (Tuckwell 1988b). Instead of these the Nagumo simplifications or

cable equations are used (Tuckwell 1988a). When collecting numerical data from these equations, we must confront them with the functional point of view. In this study we have focused on events performed in fractions of milliseconds. From this standpoint the function of both peripheral and central neurons is to transmit some signal encoded in a pulse code for a distance and then to distribute it to specific targets.

This study describes the two-point model originally introduced by Kohn (1989). It is based on the conception that the main function of the neuron is to generate pulses. The complexity of this model stands somewhere between a model with a more exact description of the membrane electricity on one hand, e.g. that of Hodgkin and Huxley and its modifications (Tuckwell 1988a; Av-Ron et al. 1993), and the leaky integrator (Tuckwell 1988a) on the other. One of the computational difficulties this model yields is that no analytical solution is known for the so-called first passage problem, i.e. the problem of estimating the time of crossing the threshold for a given random process. The non-existence of an analytical solution is not unusual in the stochastic approach and it is solved here by simulation and numerical computation. In stochastic models there is sometimes a gap between the state variables of these models and measurable biophysical values. The part of this study below equation (2) is an attempt to fill this gap. In this study the basic properties of this model are shown and then this model is applied to the description of the olfactory receptor cell.

The olfactory receptor cell is chosen here for its relative functional simplicity. In contrast to the rest of sensory pathways, the receptor cell is itself a neuron with a regular axon. Olfactory cells in vertebrates are contained in the olfactory epithelium. These cells have two ends: epithelial and axonal. The epithelial end of the cell has its surface enlarged by cilia. The odorant molecules are inhaled and passed through respiratory airways and bound to the olfactory cilia at the olfactory mucosa. This bond gives rise to the dendritic generator potential. (The generator potential can be recorded from electrodes.) The axonal end of the olfactory cell continues in the nonmyelinated fibre, the axon, ending at the next olfactory pathway relay, the olfactory bulb (Altner 1977). The changes of the dendritic potential propagate along the cell soma and increase the potential at the axon cone. When the potential at the axonal cone reaches the threshold value, it causes a neuronal firing propagating along the axon. The membrane of olfactory cilia contains protein receptors binding aromatic substances. In one olfactory cell several types of protein receptors are assumed. The olfactory cell responds to different odorants. The sensation of a particular odour arises from the activity of the mosaic of labelled lines of olfactory axons, each responding to several odorants (Altner 1977; Witkovsky 1989).

The starting point in the derivation of Hodgkin and Huxley equations is the description of ionic currents at a given membrane capacitance and different ionic

conductances:

$$C\frac{dV(x,t)}{dt} = g(V(x,t),t) \tag{1}$$

where C is the membrane capacitance, $V(x,t)$ is the membrane electric potential at a distance x and time t, and g is a net conductance as a function of the potential $V(x,t)$ and time t (Tuckwell 1988b). This model was originally identified with the results of measurements of the action potential at the axon of neurons of the giant squid. This model explains the uniformity of separate spikes of the membrane potential. Our discussion of the model presented in this paper will treat the membrane potential phenomenologically. (In conformity with the biophysical point of view, we can say that the membrane potential is a capacitor potential, discharged and charged by ionic flows, and represented in equation (1) as C).

Two-point model

In the two-point model the neuron is represented by two points or two compartments (Lánský and Rospars 1993; Kohn 1989). Let us denote the dendritic point by A and the dendritic potential by $Y(t)$, the axonal point by B and the potential by $Z(t)$, respectively. We will call $\{Y(t), t \geq 0\}$, $\{Z(t), t \geq 0\}$ processes, i.e. time-dependent functions (Tuckwell 1988b). The model can be treated as a special case of Hodgkin and Huxley equations in the following sense: instead of the continuum of values of the distance x along the axon we will substitute for x the points A and B so as to write $Y(t) \equiv V(A,t)$ and $Z(t) \equiv V(B,t)$. (This will change considerably the boundary conditions for these equations.) The potential $Y(t)$ represents the idealized collection of inputs to the cell. In our simulation example the dendritic potential $Y(t)$ is the generator potential and we will model it as a random process associated with the process of occupying protein receptors on the olfactory cell.

A striking feature of a neural cell activity is the limit frequency of spikes. The limitation of the frequency bandpass is besides other bounds given by the refractoriness of the axon to excitation immediately after the spike. The axonal refractory period in this model is reproduced by resetting the potential Z to the hyperpolarization (or, more precisely, afterhyperpolarization) level. The dendritic potential is left at its own level. The effect of afterhyperpolarization in this model is reproduced by an exponential return of the potential Z from the hyperpolarization values to the values of Y with the time constant τ. (This constant roughly corresponds to the time constant in the passive membrane model.)

Let us denote the firing threshold as S. When the potential $Z(t)$ crosses the threshold S, it elicits a unit event, an action potential. Then the function $Z(t)$ is reset to the value Y_H, which is a constant value corresponding to the membrane after hyperpolarization level. Therefore the function $Z(t)$ is discontinuous. The new passage of the potential Z over the threshold then elicits a new action potential. We will denote by Y_E the maximal excitation dendritic potential and by Y_0 the

resting dendritic potential in order that the threshold S of the point B may lie between them, $Y_0 < S < Y_E$. For the exponential return of the potential $Z(t)$ to the values of $Y(t)$ the time is counted from the last spike. The potential from the hyperpolarized level is set as a function of time from the last spike.

$$Z(t) = Y_H + \left(1 - \exp\left(\frac{t_L - t}{\tau}\right)\right) \cdot (Y(t) - Y_H) \tag{2}$$

where t is the simulation time, $t_L \leq t$ is the last spike time, τ is the membrane time constant, and Y_H is the axonal afterhyperpolarization potential, $Y_H < Y_0$. Spikes occur at moments $t_0, t_1, \ldots$, when potential $Z(t)$ crosses the threshold S, $Z(t) \geq S$. The time t_L is the nearest lower time between spikes, $t_L = t_n$ for $t_n \leq t \leq t_{n+1}$. We will define the interspike interval (ISI) as $I(n) \equiv t_{n+1} - t_n$, the average interspike interval as $EI \equiv \frac{1}{N} \sum_{n=0}^{N} I(n)$, and the average frequency as $EF \equiv \frac{1}{EI}$.

There are several possible ways of defining the dendritic potential Y. It can be treated as a noise or it can be treated as a result of a superposition of a noise and a signal. In this paper we lay stress on the potential Y as a random input.

As an example of such elementary input process we may use the Wiener process (or Brownian motion) defined as follows: $\{W(t), t \geq 0\}$ is a standard Wiener process if:
(i) $W(0) = 0$,
(ii) given any $0 \leq t_0 < t_1 < t_2 < \cdots < t_{n-1} < t_n$, the random variables $W(t_k) - W(t_{k-1})$, $k = 1, 2, \ldots, n$ are independent,
(iii) for any $0 \leq t_1 < t_2$, $X = W(t_2) - W(t_1)$ is a normal random variable with a zero mean and variance $t_2 - t_1$ (or this will be denoted $x \in N(0, t_2 - t_1)$) (Tuckwell 1988b).

The Wiener process itself is not sufficient for modelling the membrane potential, because it has no bounds. In introducing bounds for this potential, let us denote them by $W_H < W_D$ (as hyperpolarization and depolarization). When we add into the above-mentioned conditions
(iv) $W_H < W(t) < W_D$,
we shall obtain the Wiener process with a reflecting barrier (Holden 1976) where the probability distribution function of $X = W(t_2) - W(t_1)$ must be multiplied with the appropriate constant. Another difficulty is that for the values of the time interval $\Delta t = t_{k+1} - t_k$ the change of W ($\Delta W = W(t_{k+1}) - W(t_k)$) is equal to the standard deviation, $\Delta W = \sqrt{\Delta t}$, and as $\Delta t \to 0$, the velocity $\frac{dW}{dt} \to \infty$ and the trajectory becomes discontinuous. This difficulty is usually solved by the introduction of a diffusion process with a more complicated definition than the Wiener process (Lánský and Rospars 1993). The non-existence of an analytical solution of the first passage problem for a given random process was commented in the introduction. In the numerical simulation it is sufficient to consider a discrete version of the

Wiener process, the discrete random walk, (Holden 1976). We attempt to avoid too complex computation.

Our definition of the dendritic potential Y presented here is based on the model with the Poissonian excitation and Poissonian inhibition as discussed by Tuckwell (1988b). Instead of the continuous set of real numbers, the values of Y are estimated by a finite number of values in process $\{I(t), t \geq 0\}$, $I(t) \in \{1, 2, \ldots, n\}$. Let us denote the probability of incrementing $I(t)$ during the time $t \in (t_0, t_0 + \Delta t)$ p_1 (for an arbitrary t_0 and a given time step Δt), the probability of preservation of the value of $I(t)$ during this time interval p_2 and the probability of decrementing $I(t)$ p_3.

$$\begin{aligned} p_1 &= \lambda(n - I)\Delta t \qquad (I \to I + 1) \\ p_3 &= \mu I \Delta t \qquad (I \to I - 1) \\ p_2 &= 1 - (p_1 + p_3) \qquad (I \to I) \end{aligned} \tag{3}$$

The process $I(t)$ is called the birth and death process with the intensity of birth λ, and the intensity of death μ (Holden 1976). The assumption that the probabilities p_1, p_2, and p_3 are ≤ 1 can be satisfied by setting Δt sufficiently small and keeping λ and μ constant with respect to n. The probability of the just one arrival of the birth event during the time $t \in (t_0, t_0 + \Delta t)$ is $\lambda \Delta t \exp(-\lambda \Delta t)$, which has the Taylor series $\sum_{i=0}^{\infty} \lambda \Delta t(-\lambda \Delta t)^i / i! = \lambda \Delta t - \lambda^2 \Delta t^2 / 1! + \lambda^3 \Delta t^3 / 2! \ldots$. Terms with the higher order of Δt are unsubstantial for Δt small enough, $\lambda \Delta t \exp(-\lambda \Delta t)$ can be replaced by $\lambda \Delta t$. The birth event can occur $(n - i)$times and so $p_1 = \lambda(n - i)\Delta t$. And then for $\Delta t \to 0$ we can write p_1, p_2 and p_3 as in equation (3). When we use diminishing time-slices Δt, p_2 gets greater in respect to p_1 and p_3.

When simulating the process $I(t)$ we can use numerical solutions of the system of stochastic differential equations for $I'(t)$: $I'(t) = \frac{\lambda\mu}{\lambda+\mu} + \sqrt{n} U(t)$ and $\mathrm{d}U(t) = -(\lambda + \mu)U(t)\mathrm{d}t + \sqrt{\frac{2\lambda\mu}{\lambda+\mu}}\mathrm{d}W(t)$, where $W(t)$ is the Wiener process, $U(t)$ is constructed from $W(t)$ for the sake of differentiability, ($U(t)$ is the Ornstein-Uhlenbeck process), and finally $I'(t)$ approximates $I(t)$ (Kohn 1989; Lánský and Rospars 1994). In our simulation we use a method simpler than numerical solution of these equations. We simulate $I(t)$ by using probabilities p_1, p_2, p_3 from equation (3) and compare them with the output of a random number generator with uniform distribution.

The dendritic potential is set proportional to $I(t)$ and belonging to the range $Y_0 \leq Y \leq Y_E$.

$$Y(t) = (Y_E - Y_0)\frac{I(t)}{n} + Y_0 \tag{4}$$

Characteristic of the process Y

Starting from the resting-point $Y(0) = Y_0$, the mean and the variance (for $t \to \infty$) of this process will be

$$E(Y(t)) = (Y_E - Y_0)\frac{\lambda}{\lambda + \mu} + Y_0 \tag{5}$$

$$\mathrm{Var}(Y(t)) = (Y_E - Y_0)^2 \frac{\mu\lambda}{n(\lambda + \mu)^2} \tag{6}$$

When the mean potential is greater than the threshold S, it leads to neuron firing. When the passage of the process $Y(t)$ over the threshold (i.e. events $Y(t) \geq S$) is rare, or, say, when the passage occurrence tends to be the Poissonian point process, the whole cell firing will be Poissonian.

In has been pointed out that both dendritic potential and spike activity are Poissonian, if the distance of the threshold from the mean dendritic potential (normalized by its standard deviation) is greater than or equal to 3 (Lánský and Rospars 1993).

$$\frac{S - E(Y)}{\sqrt{\mathrm{Var}(Y)}} \geq 3 \tag{7}$$

Following (4) and considering that the level of S is exceeded by reaching $I(t) \geq j$, $0 \leq j \leq n$, we can substitute here for $S = \frac{j}{n}(Y_E - Y_0) + Y_0$. Then for the mean and variance from (5) and (6), (7) becomes

$$\frac{\sqrt{n}\left(\frac{j}{n}(\lambda + \mu) - \lambda\right)}{\sqrt{\mu\lambda}} \geq 3$$

and, noting that $\sqrt{\frac{\mu\lambda}{n}} > 0$:

$$\frac{j}{n}(\lambda + \mu) - \lambda \geq 3\sqrt{\frac{\mu\lambda}{n}} \tag{8}$$

As the variance (5) and the mean in (6) depend on the μ/λ ratio only, we can discuss the inequality (8) after the substitution $\mu = k\lambda$ and divided by $\lambda > 0$.

$$\begin{aligned} &\frac{j}{n}(\lambda + k\lambda) - \lambda \geq 3\sqrt{\frac{k\lambda^2}{n}} \\ &\frac{j}{n}(1 + k) - 1 \geq 3\sqrt{\frac{k}{n}} \end{aligned} \tag{9}$$

The note after equation (7) can be illustrated by setting $j = \frac{n}{2}$, which gives $(k-1) \geq 6\sqrt{\frac{k}{n}}$,

$$\sqrt{k}(\sqrt{k} - 6/\sqrt{n}) \geq 1 \tag{10}$$

This inequality for k with respect to the parameter n has then the following solution: When n is large enough (say $n > 144$), then k has to be $k > 1.7$ and this gives a relatively wide range for the ratio of input intensities, where the activity of the model neuron is Poissonian. At the other extreme of the values of the parameter n, $n < 36$, k has to be $k > 4$. This can be interpreted as follows: the less fine scale of the dendritic activation, the lesser part of the whole cell activity is Poissonian. In the simulation part, the values of λ for k close to these values will be called threshold values.

The process $I(t)$ can be generally interpreted either as excitatory and inhibitory contributions yielding reversal potentials, or, as in the following example, as receptor binding.

Application of the model to the olfactory cell

Some state variables in the model defined in preceding parts can be interpreted as biophysically measurable values at the olfactory cell. Its function was outlined in the introduction. The bond and release of an odorant at the protein receptors corresponds to the birth and death process $I(t)$. From the physiology of the olfactory cell it is known that protein receptors are joined with the G-protein whose activation opens the ion channels and raises the potential $Y(t)$. A gross simplification in the model is suggested by the assumption that the dependence of $Y(t)$ on $I(t)$ is linear. The intensity μ corresponds to the constant of releasing the odorant and λ is the intensity of odorant binding - this variable corresponds to the function of the concentration of the odorant.

The bond between an odorant and the receptors exhibits the Michaelis-Menten kinetics as a property of a small amount of receptors (represented here by the number n). The original Michaelis-Menten equation describes speed v of an enzyme catalyzed reaction as a function of the concentration c of a substrate.

$$v = \frac{V_{\max} c}{K_m + c} = V_{\max} - \frac{V_{\max} K_m}{K_m + c} \tag{11}$$

where $V_{\max}$ is the maximal speed of reaction (in other words the speed at the saturation of the enzyme system) and K_m is the appropriate Michaelis constant. Analogously, in most receptors on the cell surface, the identical functional dependence for the binding substances is described. A hormonal action can serve as a classic example. The cell response r can be expressed by the ratio to its maximal physiologically defined response:

$$r = R_{\max} - \frac{R_{\max} K_m}{K_m + c} \tag{12}$$

where $R_{\max}$ is the maximal response, c the concentration of the hormone and K_m is the appropriate Michaelis constant. For details see e.g. Murray (1990).

Chemical senses, gustation and olfaction were referred to exhibit the type of a response given by this equation (Mountcastle 1974). In case of the model olfactory cell, the acting molecules are the molecules of an odorant and the dendritic depolarization potential Y change is the physiologically defined reaction. The Michaelis-Menten kinetics is derived from the stochastic description of binding a small molecule to the protein molecule. The two-point model of a neuron is a possible generalization of this approach.

Simulation experiments and results

We have simulated this model with constants approximately close to the biological ones taking into consideration several points of view. (Implementation note: the model was written in the Turbo Pascal language. The source code was compiled with The Borland's Turbo Pascal v. 6.0 compiler and ran on a standard PC 80486 DX/40 MHz under the system MS-DOS v. 6.0. The source code is available at the author's e-mail address: MARSALEK@EARN.CVUT.CZ.) We used a Monte Carlo technique, i.e. as an input for incrementing and decrementing $I(t)$ we used calls to the pseudo-random number generator which is built in Turbo Pascal's System unit. This call returns number from range [0,1) with the uniform distribution falling into one of three intervals $[0,p_i)$, $[p_i, p_d)$ and $[p_d, 1)$, where $p_i = p_1$ and $p_d = p_1 + p_3$ for p_1, p_3 from equation (3). According to this case the appropriate transition of process $I(t)$ is chosen. All statistical tests are applied to data recorded from the moment when the model reached a steady state, i.e. the processes Y and Z stayed stationary.

For the constants of the model we substituted the following values see Table 1.:

Table 1. Parameter values of the model neuron

Parameter		Value
Y_H	Maximal hyperpolarization potential	-80 mV
Y_0	Resting potential	-70 mV
S	Threshold potential	-50 mV
Y_E	Maximal dendritic excitation potential	-30 mV
τ	Time constant	4 ms
μ	Inhibition intensity	0.0003 ms^{-1}
n	Dendritic potential scale	100

Because the process $I(t)$ (or $Y(t)$, respectively) depends only on the λ/μ ratio and the time step is always $\Delta t \leq 0.25$ ms, we can set a fixed constant $\mu =$

0.0003 ms^{-1}. The value $n = 100$ is the range of interest given by discussion of the inequality (10). For $\lambda \leq 0.039$ the note under equation (3) saying that p_1, p_2 and p_3 are probabilities is fulfilled. However, the largest λ of our interest is $\lambda = 0.02$. For λ close to μ (0.0003) is spiking very rare (E ISI is greater than 1 s), we will call these values of λ threshold values. We therefore started our investigation at the value $\lambda = 0.001$. Not surprisingly, the firing frequency (EF) exhibited a sigmoid dependence on $\log \lambda$. This curve can be compared with the steady frequency response of the olfactory cell to different concentrations of the odorant. For $\Delta t = 0.08$ and in the above described range $\lambda \in (0.0001, 0.02)$ we obtained dependence shown in Fig. 1.

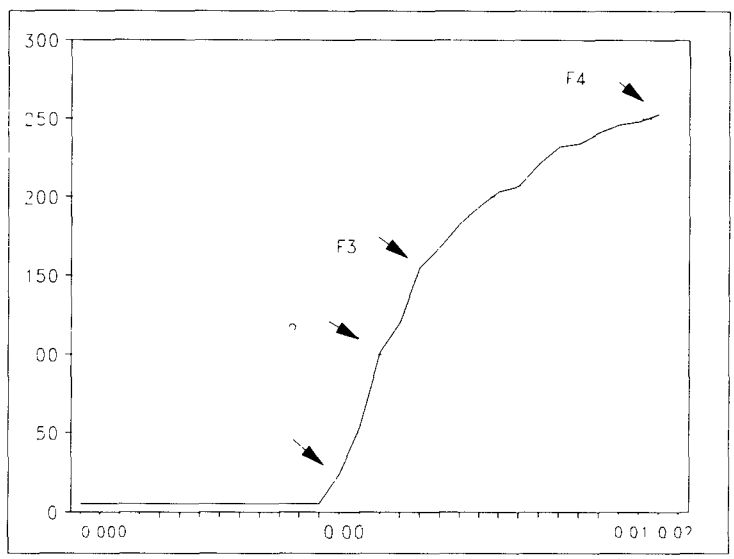

Figure 1. Simulated mean spiking frequency EF as a function of $\log \lambda$. Ranges: $EF \in (0, 300)$ [Hz], $\lambda \in (0.0001, 0.02)$ [ms^{-1}]. Model parameters used are in Table 1.

In Table 2 we have chosen points F1, F2, F3, F4 from Fig. 1 and their corresponding values of the descriptive statistics of processes $Y(t)$ and $I(t)$. Fig. 1 and Table 2 were obtained by running 1000 spikes with the appropriate parameters. The first section of this table lists for comparison the values obtained after substituting equations (5) and (6). The last column, Var ISI, shows that a high variance goes together with the higher values of ISIs, which at some point of λ gives the coefficient of variation greater than 1. This observation is typical of the Poissonian activity in spiking models.

Table 2. Dendritic potential and spiking frequencies

	Estimates after substitution into the equations (5) and (6)				
λ	Average Y EY	Variance Y Var$Y$	Average F $\dot{E}$F	Average ISI EISI	Variance ISI VarISI
0.001	-39.23	2.84	–	–	–
0.00139	-37.10	2.33	–	–	–
0.00196	-35.31	1.84	–	–	–
0.02	-30.59	0.23	–	–	–
			$\Delta t = 0.25$		
λ	EY	Var$Y$	EF	EISI	VarISI
0.001	-49.31	2.40	12.82	78.03	196009.38
0.00139	-45.56	3.33	106.50	9.39	692.63
0.00196	-42.80	1.83	149.92	6.67	0.35
0.02	-32.04	2.37	246.79	4.05	0.03
			$\Delta t = 0.08$		
λ	EY	Var$Y$	EF	EISI	VarISI
0.001	-49.23	2.60	15.42	64.86	137459.63
0.00139	-45.83	2.00	114.42	8.74	29.46
0.00196	-42.33	2.82	156.99	6.37	0.45
0.02	-32.00	2.16	252.15	3.97	0.03
			$\Delta t = 0.025$		
λ	EY	Var$Y$	EF	EISI	VarISI
0.001	-49.33	2.84	14.68	68.11	226462.87
0.00139	-46.53	3.42	84.33	11.86	1448.20
0.00196	-43.50	3.97	144.69	6.91	1.51
0.02	-31.96	2.51	255.25	3.92	0.04

The simulated mean depolarization (EY) is slightly lesser than estimated from equation (5). These values, however, agree in different simulation steps. This difference may be explained by regarding the magnitude of Δt with respect to the note under equation (3), enumerating the residuum of Taylor series as well as by considering the presumption of $t \to \infty$ in equation (5). At least, this difference does not matter with respect to the accuracy of measuring the dendritic potential. The variance Var$Y$ differs much more in this respect. Theoretically, it is indirectly proportional to λ. The simulated variance reflects rather the effects of simulation.

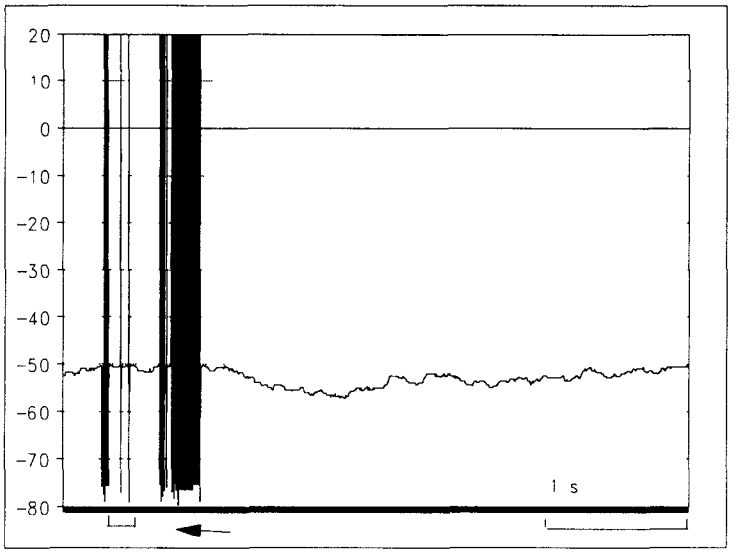

Figure 2. Example of the potential Y trace at low intensity of λ (0.001 [ms^{-1}]) and appropriate low spike rate (< 15 [Hz]). At the left there are two bursts with different duration and at the right there is a silent period. Time scale (1 s) is denoted by rectangle at the right bottom. Time interval marked by rectangle on the left (pointed out by arrow) is enlarged in Fig. 3. x-axis: time t, y-axis: potential Z; model parameters used are in Table 1.

According to Lánský and Rospars (1993), the range of suprathreshold values of λ can be divided into these sections (as shown in Fig. 1). The point F2 in Fig. 1 splits the model neuron activity into two sections (for $\lambda \leq 0.0015$ and $\lambda \geq 0.0015$). In the first section, the distribution of ISIs is exponential. This corresponds to the Poissonian spike activity. In the second section the firing activity is irregular and the distribution of ISIs can be regarded as the Gamma distribution. First section displays a very apparent bursting described in real olfactory neurons, too. In Fig. 2 there is an example of a trace of the potential Z with parameters $\Delta t = 0.025$, $\lambda = 0.001$. In the silent period (right) the traces of Y and Z are identical. The cross of Y over the threshold (marked with dotted line at the potential level equal to -50) is followed by bursts of different duration. The sample of the end of a burst from Fig. 2 is enlarged in Fig. 3 – the appropriate section is marked by a segment (the arrow on the left). In Fig. 3 the trace of the potential Y is marked by a thick and that of the potential Z by a thin curve. In Fig. 4 traces are marked in the same way as in Fig. 3. Parameters in Fig. 4 are: $\Delta t = 0.08$, $\lambda = 0.00168$. Different afterhyperpolarization is here just an artifact caused by sampling, however it reflects various onsets of successive spikes as the depolarization of Z catches up with Y.

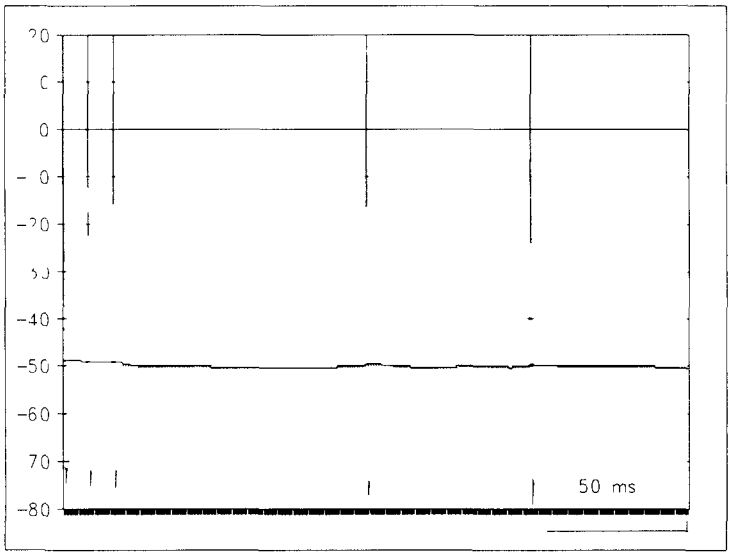

Figure 3. Enlarged example of the potential Y and Z traces at low intensity of λ and appropriate low spike rate from Fig 2 Time scale (50 ms) is denoted by rectangle at the right bottom Trace Y is denoted by thick and trace Z by thin curve Model parameters used are in Table 1

Discussion

Wiener (1958) formulated the motivation for the application of stochastic description of nature in his classical work

Computations performed by real neurons have remained up to the present time enigmatic (Witkovsky 1989) There is a general agreement on the biophysics of transmitting spikes along the axon (Tuckwell 1988a) However, no unified theory of dendritic processing has been accepted up to now (Holden 1976, Koch et al 1983, Av Ron et al 1993) Experiments and histology indicate that in different neurons dendritic processing can be quite diverse (Koch et al 1983) That is why the choice of the process Y was so detailed The birth and death process is not a unique conception for the two-point model When the main stress is attached to the information processing, the detailed description of ionic flows is abundant But once proposing neural electricity, it cannot stand in contradiction with ionic biophysics From this standpoint, different alternatives of defining dendritic potential Y can be found, (Tuckwell 1988a and 1988b, Av-Ron et al 1993, Lansky and Rospars 1993, Rospars and Lansky 1993)

One of the goals this paper pursues is to find a non-trivial description of the neuronal activity so that it might compete with other models thanks to its lesser

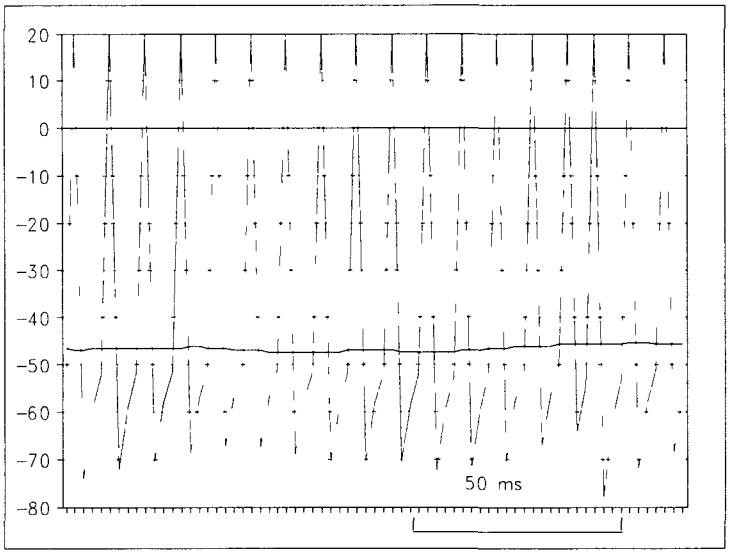

Figure 4. Example of the potential Y and Z traces at higher intensity of λ (0.00168 [ms^{-1}]) and appropriate higher spike rate ($>$ 100 [Hz]). Time scale (50 ms) is denoted by rectangle at the right bottom. Trace Y is denoted by thick and trace Z by thin curve. Model parameters used are in Table 1.

computational complexity. As compared to Av-Ron et al. (1993), Lánský and Rospars (1993), and especially Musila and Lánský (1992) (where the real time of simulation is listed), this goal was reached. The two-point or two-compartment model is not a unique solution to this problem. Tuckwell (1988b) notes a model, where the motoneuron is divided into seven compartments: three compartments for dendritic regions, soma, initial segment, first internode, and node. Differences between separate compartments are usually expressed according to their contents of different ionic channels (Tuckwell 1988b; Av-Ron et al. 1993). We will comment our two-point model as two compartments of a membrane. The natural question in the two-point model is: why is the axonal potential Z influenced by Y and not vice versa? When we assume a given distance of points A and B and for the sake of continuity of solutions of the equation (1) we presuppose that e.g. $V(x,t) = c_1V(A,t) + c_2V(B,t) = c_1Y(t) + c_2Z(t)$, for $x = c_1A + c_2B$, $c_1 + c_2 = 1$ (x being a convex combination of A and B) (regardless of the fact that the solution of equation (1) is nonlinear), the Hodgkin and Huxley equation for axon does not answer the question because it allows an orthodromic as well as an antidromic conduction due to the symmetry of boundary conditions. The question is given a valid answer only by the assumption that the neuron displays a remarkable decrease

in diameter from point A to B . Therefore the excitation is conducted only in the direction from A to B (Tuckwell 1988b). This proves an agreement of the two-point model with more detailed and experimentally confirmed models of the neural membrane.

The two-point model can be applied not only to the olfactory cell. The neurons of different populations differ in their activity and as one of their characteristics we can use the frequency spectrum. The frequency spectrum of $Y(t)$ is influenced by n and $(\lambda + \mu)$. As mentioned below equation (10), the whole model behaviour is influenced by n. This parameter will probably depend in different neurons on their functional purpose. A high n may be encountered in thalamic neurons serving as relays; a low n may be supposed in neurons with the gating function, e.g. a cat retinal ganglion (Koch et al. 1983). From this standpoint, this implies n being rather small in the olfactory cell, because it has a signal detection and amplification function. A striking phenomenon in our model is a relatively very low intensity of λ and μ. These values set large p_2 in (3) whenever Δt is small enough, and then they cause relatively slow changes of $Y(t)$ with respect to the time constant.

Another issue is the question of biological relevance. In the introduction we sketched the properties of the olfactory cell in vertebrates. We may easily compare simulated results with biological records. In several descriptions of the olfactory cell (Lánský and Rospars 1993), λ is a linear function of the concentration of an odorant. We have adopted this hypothesis. Not only in different species, but also among different cells in the same olfactory epithelium there are probably different coefficients in the linear dependency of λ on concentration and so it is reasonable to abstract from the magnitude of this coefficient. We ran the simulation for λ upper-bounded and lower-bounded. In the real olfactory cell the zero concentration has no biophysical sense and the lowest concentrations start from the concentrations of both an electrophysiological and behavioural threshold. In the range of the lower bound of the odorant concentration the olfactory cell exhibits the spiking of the so-called background activity, which is Poissonian and in several species it is approximately 5 Hz, (Mountcastle 1974; Altner 1977). The upper bound for λ is given by maximal reasonable concentrations of the odorant. A more marked simplification is yielded by the stationarity condition. The real olfactory cell works in the olfactory cycle, i.e. it is exposed to the unique air compound during one sniff cycle. The duration of the sniff cycle varies in different animals from hundreds of milliseconds to seconds. The simulation can be extended by including this cycle. The next simplification is that the threshold S is a constant. In physiology it probably rises in a sequence of events triggered by the odorant detection. This rise can be probably easily simulated by setting the threshold S as a saw-like function beginning with the rise of spiking frequency. Furthermore, on the next relay of the olfactory pathway, the signal of sniff cycle synchronization afferents surely into the olfactory bulb. A longer-term adaptation, or habituation, in the range of several

minutes, commonly observed in the olfaction, is beyond the scope of this study.

As illustrated by Figs. 2 and 3, this model reproduces bursting which is observed in real neurons and olfactory cells. A more exact modelling of bursting would involve describing the potential Y in terms of the Fourier transform. Adding the periodical function of time to the potential Y can contribute to periods of bursts. Autocorrelograms of spike trains of our model have not shown any pronounced serial correlation. A higher correlation of consecutive ISIs can be modelled by adding rectangular pulses to the Y (or joining the third point Y', corresponding to the cascade of activating G-protein in the olfactory cell (Altner 1977)).

Not less important are the implications of simulated data to the understanding olfactory pathway. Thousands of olfactory cell fibres converge into one mitral cell surrounded by the filigree lateral inhibition machinery. Thus the olfactory cell itself funtions as a detector with small n, λ and μ.

The problems and goals challenging further investigation are: What would be the adequate quantitative description of coding odour intensity for different odorants and at the higher relays of olfactory pathway? Directions are shown by Lánský and Rospars (1993). An above-mentioned extension of this model applied on the olfaction might include events accompanying the sniff cycle. Another task might be to apply the two-point or compartmental and spiking model to specimens of more complicated neural cells. An interesting perspective face to face computer hardware development is to construct nets of stochastic and spiking models and to simulate the synaptic transmission in terms of compartments.

Conclusion

One of the advantages of this approach is a relatively small computational complexity which promises in the future the tempting possibility to construct simpler neural nets of such neurons and to test quantitative hypotheses on their stochastic activity.

Acknowledgements. I would like to thank Petr Lánský for his kind reading the manuscript of my paper and his valuable suggestions and to Pavel Bělíček for language revision of my paper. This research was supported by the Internal Grant of the Charles University, number 182/1994.

References

Altner H. (1977): Physiology of Olfaction. In: Fundamentals of Sensory Physiology (Ed. R. F. Schmidt), Springer, New York

Av-Ron E., Parnas H., Segel L. A.(1993): A basic biophysical model for bursting neurons. Biol. Cybern. **69**, 87—95

Holden A. V. (1976): Models of the Stochastic Activity of Neurones. Springer, Berlin

Koch C., Poggio T., Torre V.(1983): Nonlinear interactions in a dendritic tree: Localization, timing, and role in information processing. Proc. Nat. Acad. Sci. USA **80,** 2799—2802

Kohn A. F. (1989): Dendritic transformations on random synaptic inputs as measured from a neuron's spike train - modeling and simulation. IEEE Trans. Biomed. Eng. **36,** 44—54

Lánský P., Rospars J. P. (1993): Coding of odor intensity. BioSystems **31,** 15—37

Lánský P., Rospars J. P. (1994): Ornstein-Uhlenbeck model neuron revisited. Biol. Cybern., (in press)

Mountcastle V. B. (1974): Medical Physiology. C. V. Mosby, Saint Louis

Murray J. D. (1990): Mathematical Biology. Springer, Berlin

Musila M., Lánský P. (1992): Simulation of a diffusion process with randomly distributed jumps in neuronal context. Int. J. Bio-Med. Comput. **31,** 233—245

Rospars J. P., Lánský P. (1993): Stochastic model neuron without resetting of dendritic potential: application to the olfactory system. Biol. Cybern. **69,** 283—294

Tuckwell H. C. (1988a): Introduction to Theoretical Neurobiology, part 1. Cambridge University Press, New York

Tuckwell H. C. (1988b): Introduction to Theoretical Neurobiology, part 2. Cambridge University Press, New York

Witkovsky P. (1989): Neurotransmitters and neuromodulators. In: Neuroscience (Ed. K. Walton), New York University School of Medicine, New York

Wiener N. (1958): Cybernetics or Control and Communication in the Animal and the Machine. Hermann, Paris

Final version accepted October 30, 1994